

Functional Characterization of Wild-Type and a Mutated Form of SLC26A4 Identified in a Patient with Pendred Syndrome

Silvia Dossena¹, Valeria Vezzoli¹, Nadia Cerutti⁴, Claudia Bazzini¹, Marisa Tosco¹, Chiara Sironi¹, Simona Rodighiero³, Giuliano Meyer¹, Umberto Fascio³, Johannes Fürst², Markus Ritter⁷, Laura Fugazzola⁴, Luca Persani⁴, Patrick Zorowka⁵, Carlo Storelli⁶, Paolo Beck-Peccoz⁴, Guido Bottà¹ and Markus Paulmichl^{1,2}

¹Department of Biomolecular Sciences and Biotechnology, Università degli Studi di Milano, ²Department of Physiology and Medical Physics, Medical University of Innsbruck, ³CIMA & CIMAINA, Via Celoria 26 and 16, I-20133 Milan, ⁴Department of Medical Sciences, Università degli Studi di Milano, Ospedale Maggiore IRCCS and Istituto Auxologico Italiano IRCCS, Milan, ⁵Department of Otorhinolaryngology, Medical University of Innsbruck, ⁶Department of Biological and Environmental Sciences and Technologies, Ecotekne, Università di Lecce, Monteroni, Via Provinciale per Monteroni, Lecce, ⁷Paracelsus Private Medical University, Salzburg

Key Words

Pendred syndrome • SLC26A4 • Chloride/bicarbonate exchanger • Chloride uptake • Ion transport • NPPB • DIDS • Niflumic acid

Abstract

Background: Malfunction of the SLC26A4 protein leads to prelingual deafness often associated with mild thyroid dysfunction and goiter. It is assumed that SLC26A4 acts as a chloride/anion exchanger responsible for the iodide organification in the thyroid gland, and conditioning of the endolymphatic fluid in the inner ear. **Methods:** Chloride uptake studies were made using HEK293-Phoenix cells expressing human wild type SLC26A4 (pendrin) and a mutant (SLC26A4_{S28R}) we recently described in a patient with hypothyroidism, goiter and sensorineural hearing

loss. **Results:** Experiments are summarized showing the functional characterization of wild type SLC26A4 and a mutant (S28R), which we described recently. This mutant protein is transposed towards the cell membrane, however, its transport capability is markedly reduced if compared to wild-type SLC26A4. Furthermore, we show that the SLC26A4 induced chloride uptake in HEK293-Phoenix cells competes with iodide, and, in addition, that the chloride uptake can be blocked by NPPB and niflumic acid, whereas DIDS is ineffective. **Conclusions:** The functional characteristics of SLC26A4_{S28R} we describe here, are consistent with the clinical phenotype observed in the patient from which the mutant was derived.

Copyright © 2006 S. Karger AG, Basel

KARGER

Fax +41 61 306 12 34
E-Mail karger@karger.ch
www.karger.com

© 2006 S. Karger AG, Basel
1015-8987/06/0175-0245\$23.50/0

Accessible online at:
www.karger.com/journals/net

Markus Paulmichl
Dept Biomol Sci Biotechnol, Via Celoria 26, I-20133 Milan (Italy)
or Dept Physiol Med Physics, Fritz-Pregl Straße 3, A-6020 Innsbruck (Austria)
Tel: +43-5125073756, +39-0250314947, Fax +43-512577656, +39-0250314946
E-Mail markus.paulmichl@i-med.ac.at, or E-Mail markus.paulmichl@unimi.it

Introduction

In recent years a large number of genes have been identified that are crucially involved in the genesis of human diseases, as, for instance, the SLC26A4 gene, that is involved in Pendred syndrome [1]. The SLC26A4 protein is a member of a unique family of eleven anion-transporters described so far (SLC26A1-11, A10 is reported to be a pseudogene). SLC26 proteins do transport anions, and some of them do exchange chloride for another anion, which, however, can be different with respect to the different SLC26 proteins and/or the tissue in which the particular protein members are expressed, i.e. HCO_3^- , OH^- , SO_4^{2-} , I^- , formate⁻ or oxalate⁻ [2]. The human SLC26A4 gene is located on chromosome 7 at position 7q31 and consists of 21 exons. A domain search reveals a sulfate transporter domain (pfam 00916.11), which in the case of SLC26A4 is most likely involved in chloride/anion exchange, as well as a STAS domain (pfam 01740.11). The STAS domain is located on the C-terminus of the protein and it was hypothesized that this domain could be involved in nucleotide binding [3]. The open reading frame of the SLC26A4 gene codes for a 780 amino acid protein, comprising 12 predicted transmembrane domains with both, the C-terminus as well as the N-terminus, located at the cytoplasmatic side [4, 5]. The SLC26A4 protein is mainly expressed in the thyroid gland, inner ear and the kidney and its malfunction leads to the Pendred syndrome (PS; OMIM 274600), therefore the SLC26A4 protein is also referred to as the Pendred syndrome protein. Pendred syndrome is considered one of the most common forms of syndromic deafness accounting for up to 7.5% of cases of childhood deafness [6].

More than 150 different mutations of the SLC26A4 gene have been found in humans so far (www.medicine.uiowa.edu/pendredandbor). Clinically, the patients have severe or profound sensorineural hearing loss, associated with enlargement of the vestibular aqueduct and of the endolymphatic duct and sac [7]. The hearing symptoms are associated with a positive perchlorate test, whereas goiter and hypothyroidism can be diagnosed in about half of the cases [8]. However, the detailed function of the SLC26A4 protein and the respective altered functions of the mutated SLC26A4 proteins are still elusive.

The aim of the present work was to get further insight into the function of the PDS protein in human cells. We were particularly interested in the relation between iodide and chloride transport by the protein. This issue is

of considerable clinical importance (with respect to the function of the thyroid gland) in patients with Pendred syndrome. Additionally, we were interested in testing substances that could modify the SLC26A4 induced ion transport, and therefore providing a pharmacological tool to characterize cells expressing SLC26A4 protein. Furthermore we aimed to compare the wild-type function of SLC26A4 with a mutant form of SLC26A4, i.e. SLC26A4_{S28R}, which we have recently described from a patient with Pendred syndrome. This mutation is biallelic, and associated with goiter, positive perchlorate test, hypothyroidism, severe sensorineural hearing loss, and enlargement of the vestibular aqueduct as well as of the endolymphatic duct and sac [9].

Material and Methods

Cloning of SLC26A4 cDNA

Standard procedures were used for DNA preparation, cloning, purification, and sequencing. The human wild-type SLC26A4 cDNA was obtained by RT-PCR, using total RNA from normal human thyroid tissue and Taq PLATINUM Pfx DNA polymerase (Invitrogen, Life Technologies). The SLC26A4 open reading frame was cloned into two different vectors. The first vector was pTARGET, where six histidines were added to the C-terminus of SLC26A4 for localizing the overexpressed protein by using anti-His-tag antibodies. For this procedure the primer-pair was: sense, 5'-GTT GGATCC GCG AGC AGAGAC AGG TCA-3'; antisense, 5'-CTG CGC GGC CGC TCA GTG GTG GTG GTG GTG GGA TGC AAG TGT ACG CAT A -3'. The primers contained appropriate linkers for cloning the SLC26A4 cDNA into the *Bam*H I and *Not* I sites of the pTARGET plasmid (Promega). The second vector was pIRES2-EGFP (Clontech), where SLC26A4 cDNA was subcloned, using the following primer: sense, 5'-GTA ATT ACT CGA GAG ACA GGT CAT GGC AGC G-3'; antisense, 5'-GAA TCC GGA TCC TCA AGA AGC AAG TGT ACG CAT AGC CTC-3'. For the functional studies (chloride uptake and the respective measurements of the transfection efficiency), the pIRES2-EGFP vector was used, in which the wild-type or the mutated pendrin cDNA was ligated. The use of this vector allows the simultaneous expression of two individual cDNA's from a single bicistronic mRNA without the need of physically combining the two cDNA products, i.e. to produce tandem-proteins [10]. Therefore, since EGFP expression occurs only if preceded by pendrin or mutated pendrin expression, the positive transfected cells can be individuated optically by measuring the fluorescent light emitted by EGFP. The EGFP fluorescence (Excitation maximum = 488 nm; emission maximum = 507 nm) allows to optimize the transfection procedure and to measure the transfection efficiency.

Table 1. Composition of the different extracellular solutions used for measuring the chloride uptake in the presence of high extracellular iodide concentrations.

	Standard HBSS (mM)	92 mM Iodide (mM)	92 mM Gluconate (mM)	137 mM Iodide (mM)	137 mM Gluconate (mM)
CaCl ₂ ·2H ₂ O	1.26	1.26	1.26	1.26	1.26
MgSO ₄	0.81	0.81	0.81	0.81	0.81
KCl	5.37	5.37	5.37	5.37	5.37
KH ₂ PO ₄	0.45	0.45	0.45	0.45	0.45
NaCl	136.89	45	45	-	-
NaI	-	91.89	-	136.89	-
Na gluconate	-	-	91.89	-	136.89
NaHPO ₄ ·2H ₂ O	0.34	0.34	0.34	0.34	0.34
D-glucose	5.61	5.61	5.61	5.61	5.61
HEPES	10	10	10	10	10
mannitol	20	20	20	20	20

Mutagenesis

The SLC26A4_{S28R} mutant was made using the Quik Change site-directed mutagenesis kit (Stratagene) according to the manufacturer's protocol, using the following primers: sense 5'-CGG CCG GTC TAC AGA GAG CTC GCT TTC CA-3'; antisense 5'-TGG AAA GCG AGC TCT CTG TAG ACC GGC CG-3'. The mutants were fully sequenced before testing at the functional level.

RT-PCR

Total RNA was isolated from HEK293-Phoenix and WRO cells with the Qiagen RNeasy kit as specified by the manufacturer. RNA (2 µg) was reverse transcribed by using Superscript II RT (Invitrogen). In one set of experiments, using HEK293-Phoenix mRNA, the PCR reactions were performed by using a standard Taq polymerase (Bioline), and the following primer pair: sense: 5'-CGA TGG GAA CCA GGA ATT CA-3'; antisense: 5'-TCT CAG GAC CAC AGT CAA CA-3'. The amplification product obtained was cloned into pSTBlue1 vector and sequenced (MWG Biotech, Germany). In a second set of experiments, RT-PCR analysis was performed by using both HEK293-Phoenix and WRO mRNA with the following primers [11]: SLC26A4: sense: 5'-AGC AGA GAC AGG TCA TGG CA-3'; antisense: 5'-ATC CGA CAG GAA CTG CAG CT-3', beta-actin: sense: 5'-CAC AGC TTC TCC TTA ATG TCA CG-3'; antisense: 5'-CGA GGC CCA GAG CCA AGA CA-3'. The annealing temperature was 62 °C and 32 cycles were used for amplification. These are the same conditions used by Arturi et al. [11] for semi-quantitative PCR of the pendrin mRNA.

Western-blots and membrane preparations

Cells (native HEK293-Phoenix and WRO) from a Ø 100 mm Petri dish at -80 °C were resuspended in 1 ml of buffer A (20 mM Tris-HCl pH 7.5, 150 mM NaCl, 1 mM EDTA, 1% NP40) supplemented with protease inhibitors (aprotinin, leupeptin, and pepstatin, each at a concentration of 1 µg/ml) and lysed using a syringe with a small gauge needle. Rat kidney samples were homogenized in buffer B (0.25 M sucrose, 30 mM histidine, and 1 mM EDTA, pH 7.2, supplemented with protease inhibitors, 1 ml/100 mg tissue) using a Teflon-glass Potter homogenizer. Homogenates were centrifuged at 4000 x g for 15 min at 4 °C to remove cell debris.

For membrane protein extraction, from transfected cells, we used the "Plasma Membrane Protein Extraction Kit" from MBL International Corporation following the manufacturer instructions. Protein was assayed by the Bradford method (BIO-RAD, Germany). Total (10-30 µg) and plasmatic membrane proteins (2 µg) were fractionated by SDS electrophoresis on 9% acrylamide gel and electrotransferred onto nitrocellulose membranes (Trans-Blot Transfer medium, Biorad). After treatment with PBS supplemented with 5% non-fat dry milk and 0.2% Tween 20 (Sigma), membranes were incubated overnight at 4 °C with 40 µg/ml IgG from pAb 827 kindly provided by Prof. Bernard Rousset [12]. After three washings in PBS-0.2% Tween solution, membranes were incubated for 1 h at room temperature with a 1:10000 dilution of peroxidase-coupled goat anti-rabbit antibody. Antibody-protein complexes were then detected using the ECL PLUS detection kit (Amersham Biosciences) followed by autoradiography.

Cell culture and transient transfection

HEK293-Phoenix cells (this is a second generation retrovirus producing cell line for the generation of helper free ectopic and amphotropic retroviruses) were grown in Minimum Essential Eagle Medium (Sigma) supplemented with 10% fetal bovine serum (Cambrex Bio Science), 2 mM L-glutamine, 100 units/ml penicillin, 100 µg/ml streptomycin and 1 mM pyruvic acid (sodium salt). WRO cells (this is a human cell line derived from a follicular carcinoma; [13]) were grown in Dulbecco's modified Eagle's medium (Sigma), supplemented with 2 mM L-glutamine, 1 mM pyruvic acid, 100 units/ml penicillin, 100 µg/ml streptomycin and 10% fetal bovine serum. The cells were maintained at 37 °C in a 5% CO₂:95% air humidified incubator; subcultures were routinely established every second to third day by seeding cells in Petri dishes (Ø 100 mm) after trypsin/EDTA treatment.

For uptake experiments, cells were transiently transfected with wild-type SLC26A4 or SLC26A4_{S28R} (both cloned into pIRES2-EGFP plasmids); negative controls were performed on cells transfected with empty plasmid (pIRES2-EGFP only). The day before transfection, cells were seeded in poly-L-lysine-treated 24-well plates and grown to 60% to 80% confluency. HEK293-Phoenix cells were transfected by calcium phosphate precipitation; for each well, 0.9 µg of plasmid dissolved in 13.5

µl of water were mixed with 1.5 µl of buffer A (2.5 M CaCl₂, pH 5.8) and with 15 µl of buffer B (140 mM NaCl, 1.5 mM Na₂HPO₄, 50 mM HEPES, pH 7.05 adjusted with NaOH). WRO cells were transfected by using Metafectene (BionTex); for each well, 1 µg of plasmid dissolved in 30 µl of culture medium (without serum and antibiotics) was mixed with 3 µl of Metafectene dissolved in 30 µl of the culture medium as described above. After an incubation of 20-30 min at room temperature (HEK293-Phoenix and WRO), the transfection mix was spread over the cells; after 8-10 hours, the cells were washed twice with fresh culture medium.

For immunocytochemistry, cells were seeded on glass coverslips (Ø 10 mm) and transfected as previously described with the pTARGET vector coding for wild-type SLC26A4 or SLC26A4_{S28R}, or with the empty plasmid (negative controls). For co-localization studies, cells were co-transfected with wild-type SLC26A4 or SLC26A4_{S28R} and pEYFP-mem (Clontech) plasmids (1:1 ratio).

Chloride uptake studies

The cells were seeded and transfected as described above, and used for uptake experiments 30 hours after transfection. Usually, cells were washed at room temperature with 2 ml of incubation buffer (Hanks' balanced salt solution; Sigma) supplemented with 10 mM HEPES and 20 mM mannitol, and then incubated for 2 min with 300 µl of the same buffer supplemented with 3-4 mM ³⁶Cl⁻ (specific activity 2 µCi/ml). After incubation, cells were washed three times with 2 ml of ice-cold incubation buffer and solubilized with 300 µl 0.1 M NaOH, 0.1% (wt/vol) sodium dodecyl sulfate and 2% Na₂CO₃; the lysate was centrifuged at 4000 rpm for 10 min, and the radioactivity in the supernatant was counted by liquid scintillation spectrometry (1600 TRI-CARB liquid scintillation analyzer, Packard). For iodide competition experiments, the incubation buffer was modified as specified in Table 1; where indicated, inhibitors were dissolved in DMSO and added to the incubation buffer at the appropriate final concentration. The total protein content of cells in each well was measured by Bradford method and used for normalization of the chloride uptake (expressed as pmol Cl⁻/µg protein). The uptake experiments were made, as described above, after 2 minutes of incubation with ³⁶Cl⁻. It is important to note, that within this time frame (data points at 10, 30 and 120 seconds) the ³⁶Cl⁻ uptake in HEK293-Phoenix and WRO cells is linear (data not shown), suggesting an unidirectional (inward directed) flux of chloride, which therefore is not contaminated by a ³⁶Cl⁻ efflux [14]. To determine non-specific binding, chloride uptake was measured in SLC26A4 transfected HEK293-Phoenix cells (n=40) and in control cells (n=40) after 10 seconds and 2 minutes of incubation; uptake kinetics were interpolated by linear regression, and the theoretical uptake at time 0 (non-specific binding) was calculated as intercept on the y-axis. Non-specific binding was not statistically different between SLC26A4 transfected cells and control cells, and was 127±31 pmol Cl⁻/µg protein (n=80). The specific uptake obtained in every experiment has been corrected for this value (for WRO cells the non-specific binding was 32±11 pmol Cl⁻/µg protein; n=10).

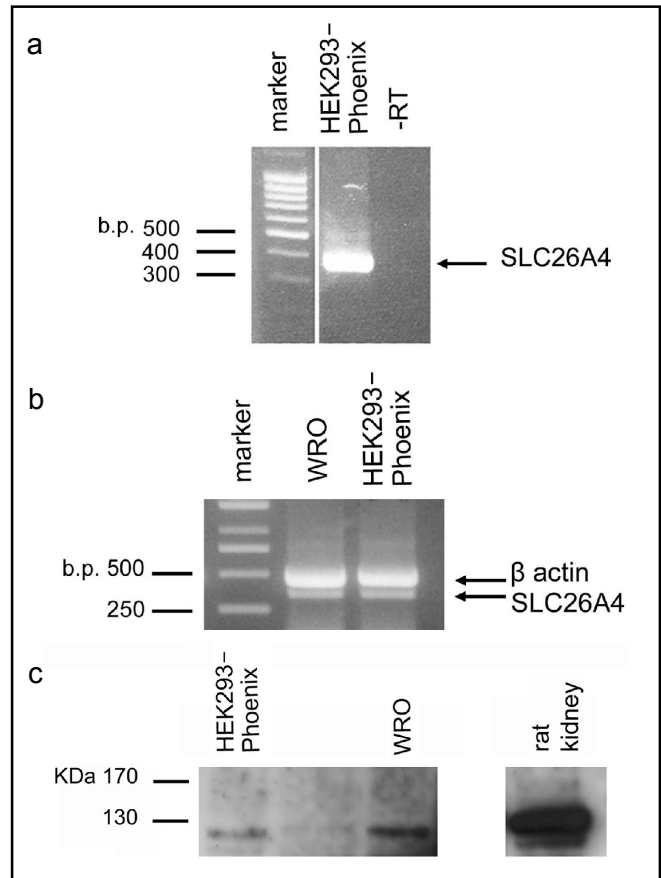


Fig. 1. SLC26A4 is expressed in HEK293-Phoenix and WRO cells. (a) RNA was prepared from HEK293-Phoenix cells and subjected to reverse-transcription (for the primer pair, see Material and Methods). The specificity of the reaction was controlled by sequencing the amplification product. (b) RT-PCR of SLC26A4 in HEK293-Phoenix and WRO cells. The amount of SLC26A4 mRNA in both cell systems seems to be similar if compared to the mRNA of β-actin. (c) SLC26A4 protein is expressed in both cell types (the western-blot of rat kidney SLC26A4 is added as a size control).

Immunocytochemistry and co-localization

For the immunofluorescence assays, cells were washed 30 hours after transfection with 2 ml PBS at room temperature, fixed for 15 min in 3% paraformaldehyde, permeabilized for 3 min with 0.1% Triton X-100 and blocked 1 hour at room temperature in PBS/3%BSA. For immunocytochemistry experiments, coverslips were incubated overnight at 4 °C with Alexa Fluor 488 coupled anti His-tag mouse monoclonal antibody (Penta His™ Alexa Fluor® 488 Conjugate, Qiagen, Germany) diluted 1:400 in PBS/0.1%BSA. For co-localization studies EYFP-mem was used. This is a fusion protein consisting of the N-terminal 20 amino acids of neuromodulin, also called GAP-43, and a yellow-green fluorescent variant of the enhanced green fluorescent protein (EGFP). Expression of EYFP-mem in mammalian cells results in strong labelling of plasma membrane; however, during the different steps of its trafficking, it also

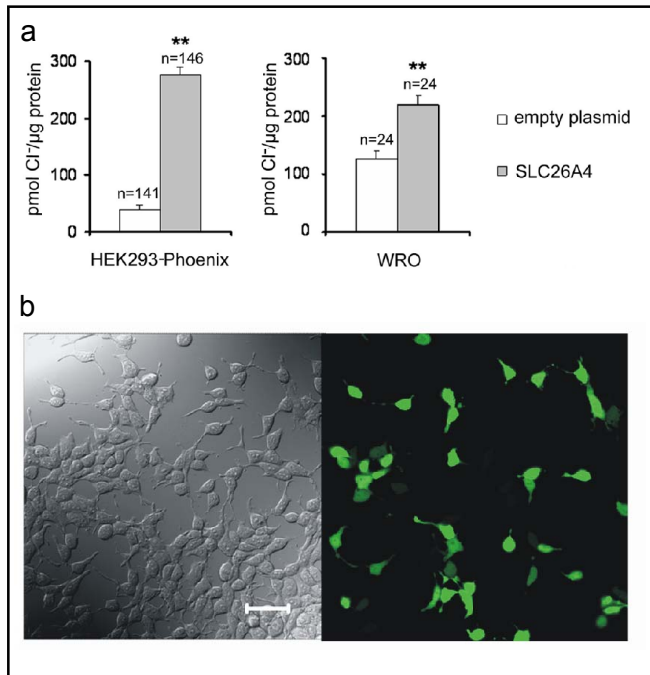


Fig. 2. Chloride uptake in HEK293-Phoenix and WRO cells over-expressing SLC26A4. (a) The chloride uptake is given 2 minutes after incubating the cells with the radioisotope ($2 \mu\text{Ci/ml } ^{36}\text{Cl}^-$). Control-experiments were made by using cells transfected with the empty plasmid expressing solely EGFP. The expression of SLC26A4 leads to a sevenfold increase of the chloride uptake in HEK293-Phoenix cells (left panel). The increase of chloride uptake in WRO cells (right panel) was smaller if compared with HEK293-Phoenix cells, most likely due to the lower transfection efficiency obtained in WRO cells if compared to HEK293-Phoenix cells (see text). For these and all subsequent chloride flux measurements, the non-specific binding (see Material and Methods) was subtracted from the respective values. (b) The transfection efficiency was measured by the simultaneous expression of SLC26A4 and EGFP by using an IRES-vector (here shown for HEK293-Phoenix cells; see also Material and Methods). On the left the transmission image is given, on the right, the respective green fluorescence (EGFP) in the positively transfected cells. Scale bar: $50 \mu\text{m}$. (**= $p < 0.001$).

partially labels intracellular membranes. After (50 hours) double transfection with pTARGET-SLC26A4 and pEYFP-mem plasmids, cells were treated as described above, and incubated overnight at 4°C with anti His₆ mouse monoclonal antibody (Roche) diluted 1:100 in PBS/0.1%BSA. Then, coverslips were washed three times in PBS and incubated for 2 hours at room temperature with Alexa Fluor 568 coupled goat anti-mouse secondary antibody (Invitrogen) diluted 1:100 in PBS/0.1%BSA.

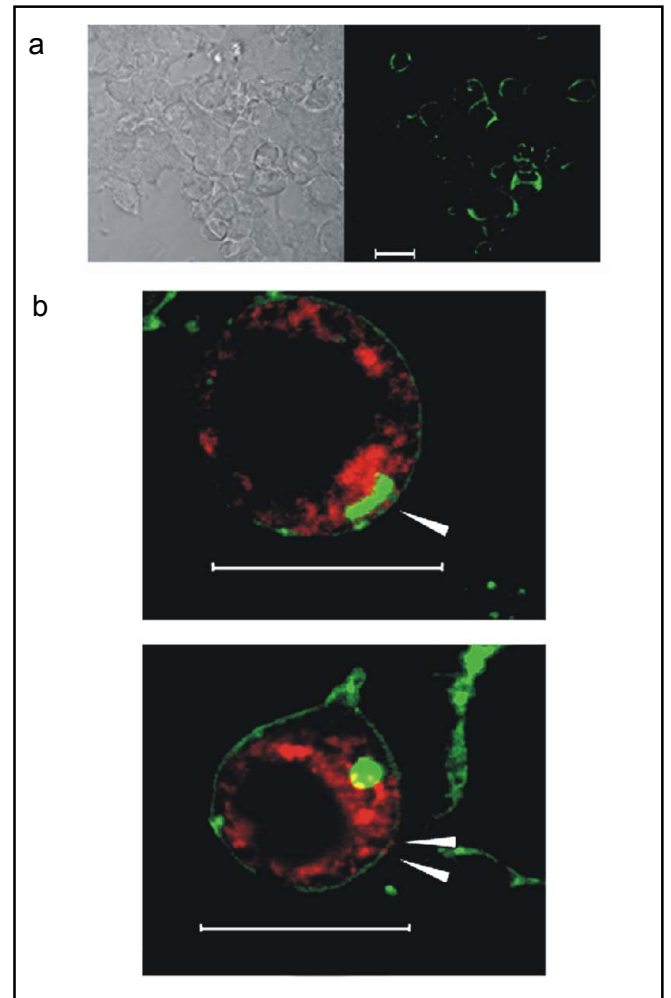
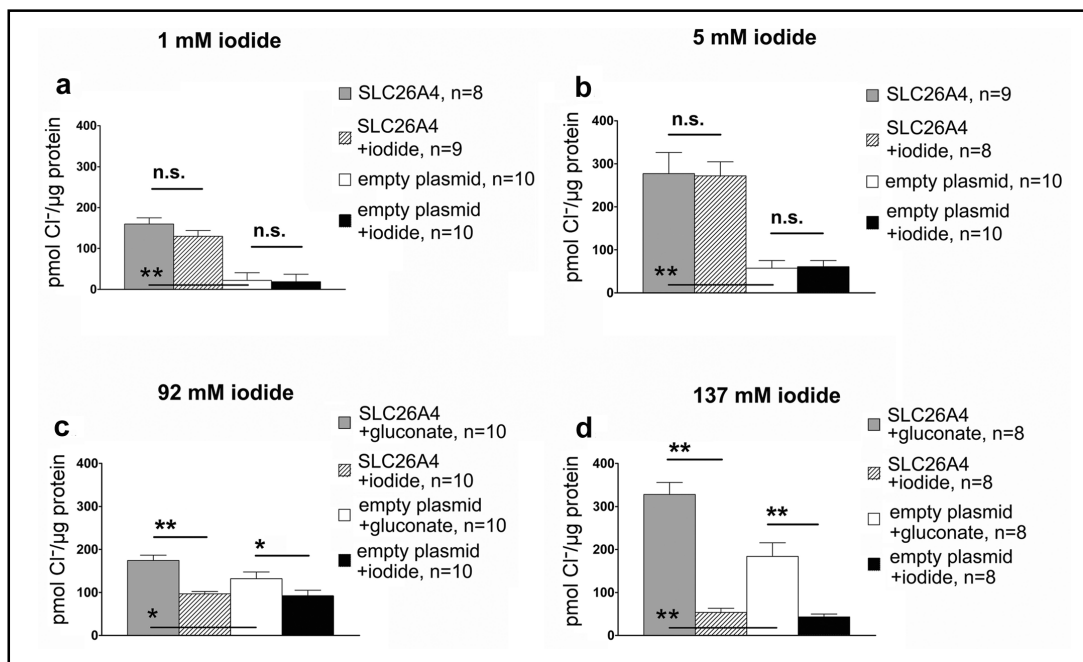


Fig. 3. Expression of exogenous SLC26A4 in HEK293-Phoenix cells. (a) The His-tagged SLC26A4 was visualized by using anti-His-tag antibodies. In these experiments SLC26A4 was not coexpressed with EGFP. On the left panel the transmission image is given, on the right the respective confocal image of the fluorescence of the anti-His-tag antibody (labelled with Alexa 488; green signal); scale bar: $20 \mu\text{m}$. (b) The subcellular localization was done by co-expressing His-tagged SLC26A4 (Alexa 568; red signal) together with EYFP-mem, a EYFP conjugated membrane label (green signal). Two different cells are shown, and the arrows indicate membrane bound SLC26A4; scale bar: $16 \mu\text{m}$.

Conventional and confocal microscopy

Transfection efficiency was determined by visualizing EGFP transfected cells with an inverted microscope (Axiovert 135, Zeiss) equipped for incident-light fluorescence with a xenon lamp (XBO 75 W) and 09 series Zeiss filters. Fluorescence images were obtained with a Leica TCSNT confocal microscope; focal series of horizontal planes of section were monitored using an Ar/Kr laser (blocking filter BP 530/30 for Alexa Fluor 488, EGFP, EYFP; blocking filter LP 590 for Alexa Fluor 568).

Fig. 4. Iodide competition of chloride uptake in HEK293-Phoenix cells. The chloride uptake was measured by adding 1 mM and 5 mM sodium-iodide to the extracellular solution, respectively (a and b), and the respective values were corrected for the unspecific binding. In addition, the chloride uptake was measured by substituting 92 mM or 137 mM of NaCl with respective amounts of sodium-iodide, or sodium-gluconate (c and d; these values were not corrected by the unspecific binding, which was determined at an extracellular chloride concentration of 135 mM chloride); n.s. = non significant, * = $p < 0.05$, and ** = $p < 0.01$.



these values were not corrected by the unspecific binding, which was determined at an extracellular chloride concentration of 135 mM chloride); n.s. = non significant, * = $p < 0.05$, and ** = $p < 0.01$.

Drugs and chemicals

NPPB (5-Nitro-2-(3-phenylpropylamino)benzoic acid), DIDS (4,4'-Diisothiocyanatostilbene-2,2'-disulfonic acid disodium salt hydrate), niflumic acid, DMSO (Dimethyl sulfoxide) and all salts were purchased from Sigma (St Louis MO, USA). $^{36}\text{Cl}^-$ (sodium chloride solution) was obtained from Amersham, UK; OptiPhase 'HiSafe' 3 liquid scintillation cocktail was from Perkin Elmer.

Statistical Analyses

Data are expressed as arithmetic means \pm S.E. Statistical analysis was made by the unpaired or, where applicable, paired *t* test. Statistically significant differences were assumed at $p < 0.05$.

Results

Endogenous SLC26A4 expression in HEK293-Phoenix and WRO cells

The SLC26A4 protein is expressed under native conditions in the kidney [15-20], and here we show, using RT-PCR, that the SLC26A4 is, in addition, expressed in human-embryonic-kidney (HEK293-Phoenix) cells. The amplification product is shown in figure 1a. The specificity of the approach was proven by sequencing the amplification product. This procedure confirmed that the obtained DNA sequence from HEK293-Phoenix cells corresponds to the sequence of human SLC26A4 (data

not shown). Similarly, the transcription of SLC26A4 mRNA was also proven in WRO cells, a cell-line derived from the human thyroid (figure 1b). RT-PCR, suggested similar transcription levels of SLC26A4 in HEK293-Phoenix and WRO cells (figure 1b). These results were reconfirmed by Western-blots using anti-pendrin antibodies (pAb 827 IgG; kindly provided by B. Rousset [12]) demonstrating that in both cell lines the SLC26A4 protein is indeed expressed (figure 1c).

SLC26A4 overexpression in HEK293-Phoenix and WRO cells leads to an increased chloride uptake

As shown in figure 2a, the overexpression of SLC26A4 leads to a high, and statistically significant, increase of the chloride uptake. If compared to HEK293-Phoenix cells expressing only the reporter EGFP protein, the chloride uptake in cells expressing both, EGFP as well as SLC26A4 (two separate proteins, see material and methods) is sevenfold increased, i.e. the chloride uptake increases from 39 ± 7 pmol chloride / μg protein ($n=141$) to 276 ± 14 pmol chloride / μg protein ($n=146$). The transfection efficiency in our experiments was $54.7 \pm 3.7\%$ ($n=27$) measured by fluorescence means, determining the number of cells showing the signal induced by EGFP (figure 2b), therefore the sevenfold increase of chloride uptake underestimates the real effect induced

by the expression of the SLC26A4 protein. In WRO cells, overexpression of SLC26A4 leads to an increase of chloride uptake from 125.7 ± 14.9 pmol chloride/ μg protein in control cells ($n=24$), to 218.9 ± 16.7 pmol chloride/ μg protein in SLC26A4 expressing cells ($n=24$), respectively. For the latter, the transfection efficiency was 5-10%, which is significantly lower if compared to HEK293-Phoenix cells, and could therefore explain the weaker increase of chloride uptake observed in WRO cells.

Expression and subcellular localization of exogenous SLC26A4 in HEK293-Phoenix cells

Western-blot experiments using HEK293-Phoenix cells demonstrated that the transfection of SLC26A4 as well as of the SLC26A4_{S28R} mutant leads to an overexpression of the respective protein (see below). Furthermore, the expression of exogenous SLC26A4 in HEK293-Phoenix cells was verified by immunocytochemistry and visualized by using a His-tagged form of the protein (figure 3a). The His-tag was added to the C-terminus, which is located in the cytosol [4, 5]. At the sub-cellular level, SLC26A4 immunoreactivity is highest in cytoplasmic vesicles (figure 3b). However, as shown in figure 3b, a fraction of the expressed protein is located at the level of the cytoplasmic membrane, the functional compartment of the anion exchanger. This finding is substantiated by Western-blots using plasma membrane preparations of HEK293-Phoenix cells (see figure 6c).

Iodide competes with chloride for the uptake

It has been shown, that besides chloride, the SLC26A4 protein is also able to transport I^- , HCO_3^- , OH^- and formate $^-$ [20-22]. The HCO_3^- , formate, OH^- , as well as chloride transports were also verified by expressing the SLC26A4 protein in HEK293-Phoenix cells [20]. Here we characterize for the first time the influence of iodide on the chloride uptake in HEK293-Phoenix cells. As shown in figures 4a and b, neither the addition of 1 mM nor 5 mM iodide to the extracellular fluid is able to significantly change the chloride uptake. In order to test higher concentrations of iodide, i.e. 92 mM or 137 mM, we substituted extracellular unlabeled chloride with gluconate or with iodide. This procedure was chosen to prevent osmotic perturbations after adding iodide and to unmask the iodide effect. As shown in figures 4c and d, the presence of 92 mM or 137 mM iodide leads to a marked and significant reduction of chloride uptake (from 174 ± 12 pmol chloride/ μg protein ($n=10$) to 97 ± 5 pmol chloride/ μg protein ($n=10$), and from 328 ± 28 pmol

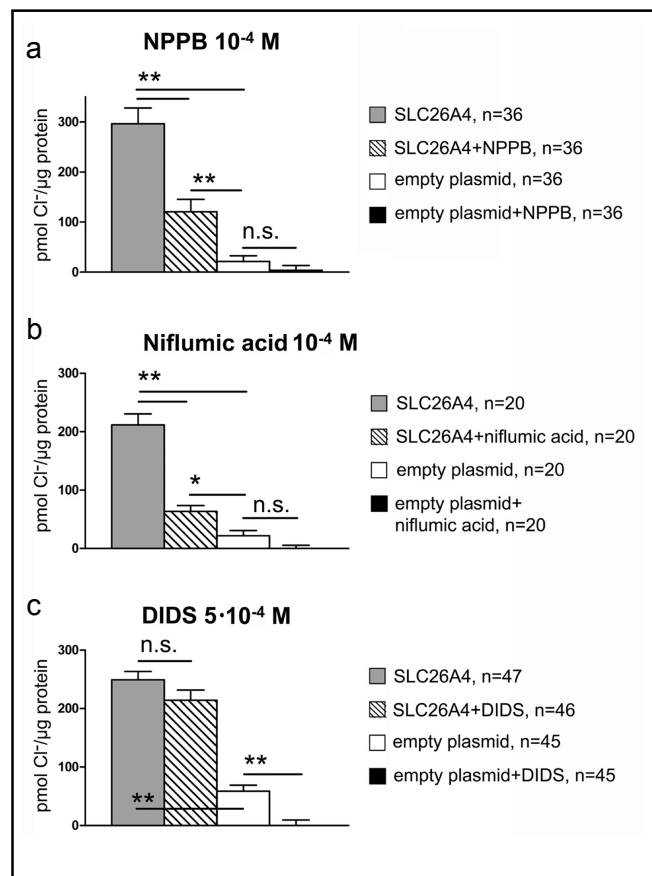


Fig. 5. Chloride uptake in HEK293-Phoenix cells measured in the presence of known chloride-transport blockers. NPPB (0.1 mM; a), as well as niflumic acid (0.1 mM; b), are able to reduce SLC26A4 induced chloride uptake. DIDS (0.5 mM; c) is not able to reduce SLC26A4 induced chloride uptake, however, the chloride uptake in control cells can be blocked by the drug; n.s. = non significant, * = $p < 0.05$, and ** = $p < 0.01$.

chloride/ μg protein ($n=8$) to 54 ± 10 pmol chloride/ μg protein ($n=8$), for 92 mM and 137 mM iodide respectively) to an amount, which is indistinguishable from the uptake in the presence of the respective amount of iodide in control cells (92 ± 13 pmol chloride/ μg protein ($n=10$), and 43 ± 6 pmol chloride/ μg protein ($n=8$), for 92 mM and 137 mM iodide, respectively). These results are in accordance with the hypothesis that iodide, like chloride, can be transported by SLC26A4.

In the control cells, which are not transfected with SLC26A4, iodide, as described above, is again able to reduce significantly the chloride uptake (figure 4c and d). A possible explanation for this finding is that iodide also competes with the endogenous Cl^- transport systems, that contribute to the overall Cl^- uptake in these cells (figure 5c).

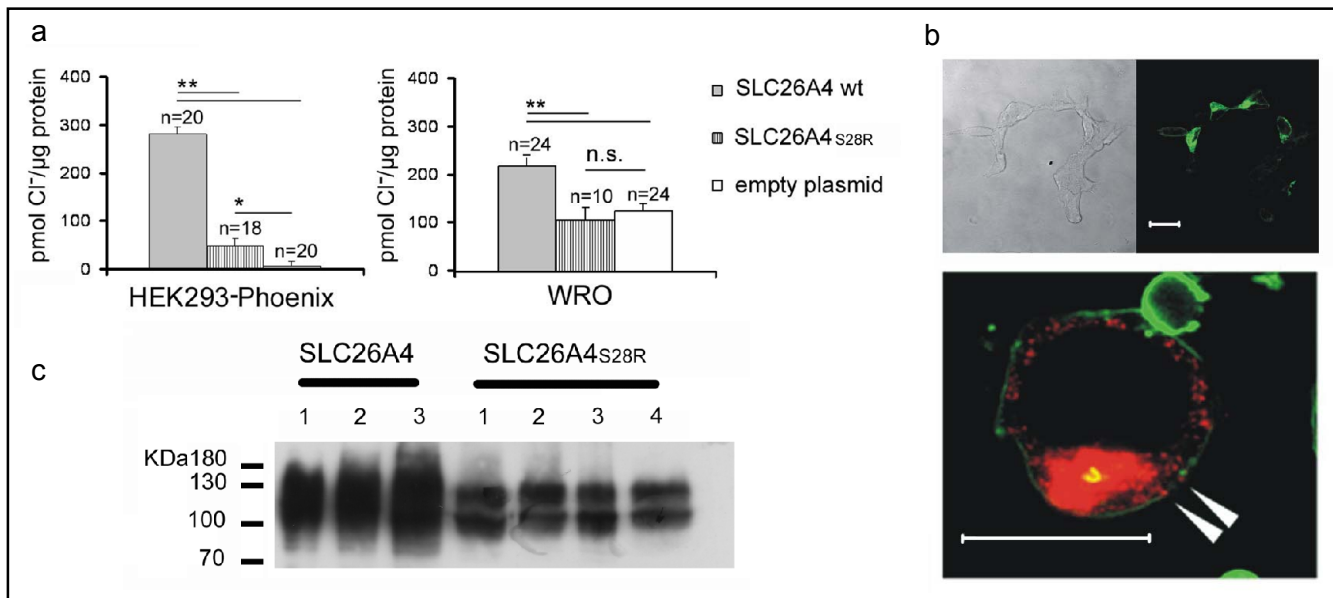


Fig. 6. Functional characterization of the SLC26A4_{S28R} mutant of SLC26A4 in HEK293-Phoenix as well as WRO cells. (a) The chloride uptake of SLC26A4_{S28R}, compared to wild-type, is markedly reduced, if expressed in both, HEK293-Phoenix or WRO cells. (b) The expression pattern of SLC26A4_{S28R} is similar to wild-type SLC26A4 (see figure 3). On the upper left side, the transmission image is given, the corresponding fluorescence image, obtained from the anti-His-tag antibody is shown on the right side (the green signal indicates the SLC26A4 expression); scale bar: 20 μ m. Below, the co-localization of SLC26A4_{S28R} (red signal), and EYFP-mem (green signal) are given; scale bar: 16 μ m (for details, see figure 3). (c) Both, wild-type SLC26A4 as well as the tested mutant are expressed at the level of the plasma membrane. Western-blot of wild-type (SLC26A4; three different preparations) and mutant SLC26A4 (SLC26A4_{S28R}; four different preparations) in isolated plasma membranes are shown. (n.s. = non significant, * = $p < 0.05$, and ** = $p < 0.01$).

SLC26A4 dependent chloride uptake can be blocked by NPPB, and niflumic acid but not by DIDS

NPPB as well as niflumic acid are known blockers of chloride transport in a variety of different cells [23-25]. The chloride uptake in cells over-expressing the pendrin protein was tested in the presence of both substances (figure 5a and b). Both blockers applied at concentration of 0.1 mM, are able to reduce the chloride uptake, i.e. by $59.3 \pm 8.4\%$, $n=36$ (NPPB; 0.2% DMSO; DMSO alone has no effect on the chloride uptake, data not shown) and $69.9 \pm 4.5\%$, $n=20$ (niflumic acid; 0.1% DMSO). In contrast, 0.5 mM DIDS (0.5% DMSO) is not able to significantly impair the SLC26A4 induced chloride uptake ($n = 46$), whereas the chloride uptake in control-cells not over-expressing SLC26A4 is completely blocked ($n = 45$).

Functional characterization of a mutated (S28R) SLC26A4 protein

As shown in figure 6a, the chloride uptake measured in HEK293-Phoenix cells expressing the mutated form

of SLC26A4 (SLC26A4_{S28R}) is markedly reduced (by $\sim 80\%$), if compared to HEK293-Phoenix cells expressing the wild-type form of SLC26A4 (from 281 ± 14 pmol chloride / μ g protein ($n=20$) to 48 ± 16 pmol chloride / μ g protein ($n=18$), respectively). The transfection efficiency of SLC26A4_{S28R} transfected HEK293-Phoenix cells (54.6 ± 4.5 , $n=28$) is statistically not different to wild-type SLC26A4 transfected HEK293-Phoenix cells. Similarly the chloride uptake was also measured in WRO cells expressing wild-type or mutant SLC26A4. As in the case of HEK293-Phoenix cells, the chloride uptake measured in WRO cells expressing SLC26A4_{S28R} is markedly lower if compared to WRO cells expressing wild-type SLC26A4 (107 ± 24.5 pmol chloride / μ g protein; $n=10$, and 218.9 ± 16.7 pmol chloride/ μ g protein; $n=24$, respectively) and not significantly different from control WRO cells (125.7 ± 14.9 pmol chloride / μ g protein; $n=24$). The expression pattern of SLC26A4_{S28R} is indistinguishable from the pattern of wild-type SLC26A4 (figure 6b). Western-blot experiments confirmed that significant amounts of SLC26A4_{S28R} protein could be detected at the plasma membrane level (figure 6c).

Discussion

Despite the obvious clinical relevance of SLC26A4, the detailed function of the SLC26A4 transporter is still elusive, particularly in respect to its function in different organs in which it is expressed. In the inner ear SLC26A4 is expressed in the cochlear external sulcus cells, vestibular transition cells and endolymphatic sac cells [26, 27]. These cells are involved in the conditioning of the endolymphatic fluid and in these cells the SLC26A4 transporter is most likely acting as a $\text{Cl}^-/\text{HCO}_3^-$ exchanger. In the kidney, SLC26A4 is located in the apical membrane of β -intercalated cells [17-19]. There, SLC26A4 seems to be involved, amongst other important transporters like AE1 and AE4 [28-30] in bicarbonate transport, which is activated in metabolic alkalosis and inactivated in metabolic acidosis [19, 31], most likely by a process called 'plasticity of epithelial polarity' [32, 33]. In the thyroid gland, SLC26A4 is expressed in the thyrocytes, where it has been shown that SLC26A4 resides in the apical membrane [4]. This membrane is facing the follicular lumen into which the exchanger is supposed to transport iodide that will then be organified on thyroglobulin. Thyroglobulin, after reabsorption into the thyrocytes, will be modified by lysosomal degradation and transformed to thyroid hormones [34, 35].

The aim of the present study was to compare, on a functional level, wild-type SLC26A4 with a mutant form (SLC26A4_{S28R}). Several different studies were made using the expression of the SLC26A4 protein in non-polarized human-embryonic-kidney (HEK) cells [20, 36, 37], claiming, that the SLC26A4 protein is not expressed in those cells [4, 20]. Here we show, that the SLC26A4 protein is expressed in non polarized HEK293-Phoenix as well as in non-polarized WRO cells [13], and therefore we can assume that these cells also possess the environment needed for SLC26A4 function (despite the fact that the cells we use are not polarized). This is particularly important for the present study, since we would like to investigate a mutated form of SLC26A4, i.e. SLC26A4_{S28R}, which bears the mutation in the N-terminal, i.e. the cytoplasmatic part of the protein [4]. The use of cell lines that are able to functionally express the SLC26A4 protein are therefore advantageous for the functional comparison of wild-type and mutated transporter.

In both non-polarized cell lines, i.e. HEK293-Phoenix and WRO, the expression of SLC26A4 leads to an increased chloride uptake, which is in agreement with the hypothesis, that the protein acts as a chloride-

transporter [19, 20]. From the experiments reported here, however, we can not speculate whether the transporter is electroneutral or electrogenic as proposed by Ko [38] and Yoshida [39]. However, we recently showed, that SLC26A4 expressed in HEK293-Phoenix cells is electroneutral [40].

At the sub-cellular level, SLC26A4 immunoreactivity is highest in cytoplasmic vesicles of the cell line tested. This finding is well in agreement with previous observations in kidney cells [16, 18, 41-43] and endometrium [44], using antibodies against pendrin. The localization of wild-type or mutated SLC26A4-GFP was also reported in non-polarized HeLa cells [36], as well as COS7 and FRTL5 cells. In the latter study, different cytosolic expression patterns of wild-type SLC26A4 were observed, depending on the cell line used. Whereas in COS7 cells the subcellular expression was located predominantly at the endoplasmatic reticulum, the subcellular expression in FRTL5 cells is located at the Golgi complex [45]. The subcellular expression pattern seems therefore to depend on the cell type used, and is most likely the result of the slow-folding process involved in SLC26A4 overexpression, leading therefore to aggregate formation [46]. However, in all studies reported so far, including the present, SLC26A4 can also be individuated at the level of the cell membrane which corresponds to the functional compartment of the anion-exchanger.

It has been shown, that besides chloride, the SLC26A4 protein is also able to transport I^- , HCO_3^- , OH^- and formate [20-22]. The vectorial transport of iodide by pendrin has been demonstrated in polarized cells [5]. Conflicting reports are reported about a possible competition between iodide and chloride on the transport level of SLC26A4. Whereas Yoshida and collaborators do not observe such a competition [47], the expression of human SLC26A4 in both *Xenopus* oocytes and Sf9 cells seems to mediate chloride as well as iodide transport [21]. In accordance to the latter study, our results obtained in experiments in which chloride was substituted by iodide are in accordance with the hypothesis that iodide can indeed be transported by SLC26A4.

So far only some of the known blockers of anion transporters have been tested on SLC26A4, i.e. DIDS, furosemide and probenecid, which lead to a relatively weak ion-transport inhibition [21, 48]. Therefore we investigated the effects of additional inhibitors, which have so far not been tested on SLC26A4 before, and could thus help to develop a pharmacological 'fingerprint' of the SLC26A4 function. This is the first time that niflumic

acid or NPPB were tested in SLC26A4 expressing cells, and we show, that both blockers applied at concentration of 0.1 mM, are able to reduce the chloride uptake. It was reported, that micro-molar concentrations of niflumic acid are able to reduce the SLC26A3 (DRA) induced ion transport. DRA is the most similar SLC26 protein to pendrin (45% amino acid identity), and whose inhibition by DIDS is controversial [49]. It is important to note, that in our experiments, 0.5 mM DIDS is not able to impair the SLC26A4 induced chloride uptake, whereas the chloride uptake in control cells not over-expressing SLC26A4 is completely blocked. This underlines the assumption, that in control cells, under the conditions used, the chloride uptake in the absence of pendrin over-expression is mainly supported by transporters other than SLC26A4, which are DIDS sensitive. So far the DIDS sensitive chloride uptake in cells over-expressing SLC26A4 was only tested in oocytes [21]. In contrast to our finding, in the latter, the pendrin induced chloride uptake was sensitive to DIDS. The different cellular system in which the SLC26A4 was over-expressed, and in addition the fact that the DIDS effect was studied in the virtual absence of extracellular chloride, or the higher DIDS concentration (1 mM) used in the oocyte study, might explain the observed discrepancy. Defining the functional pattern of SLC26A4 modulators can help to provide a pharmacological tool for characterizing the involved transport pathways.

Recently we have described a mutation in the SLC26A4 protein associated with goiter and positive perchlorate test, hypothyroidism, and severe sensorineural hearing loss, associated with enlargement of the vestibular aqueduct and of the endolymphatic duct and sac [9]. The patient showed a biallelic missense mutation in exon 2 leading to the substitution of a serine for an arginine (SLC26A4_{S28R}). The parents of the patient showed the same mutation in heterozygous form [9]. No chloride uptake studies of SLC26A4 mutants are described so far in human expression systems. The three mutants described by Rotman-Pikielny and collaborators were all retained in the subcellular compartment [45] and in this study no functional assays were used. Taylor and collaborators investigated the iodide efflux in cells co-expressing SLC26A4 mutants together with NIS, a known sodium/iodide cotransporter [50, 51]. Most of the mutants used in this study displayed complete loss of pendrin induced iodide transport [36]. Scott and collaborators tested the chloride and iodide uptake of SLC26A4 mutants

expressed in *Xenopus laevis* oocytes [52], and compared the respective uptakes with oocytes expressing wild-type pendrin. For three mutants associated with Pendred syndrome (T416P, L236P and E384G) no different chloride or iodide uptake could be observed compared to control cells, however, for mutants observed in patients with non-syndromic hearing loss (DFNB4; I490L, G497S, V653A and V480D), the chloride as well as iodide uptake was reduced. These studies clearly demonstrate the need for functional studies of the transport features of SLC26A4 mutants in mammalian expression systems. Here we show, that SLC26A4 and the S28R mutant we used are transposed towards the membrane, and that the mutation leads to a marked reduction of the transport capabilities of the ion exchanger. The mechanism by which the S28R mutation is leading to the observed reduced chloride transport is not clear yet. Further studies are needed for getting detailed insight into the involved mechanisms.

Conclusions

The SLC26A4 protein is a chloride/anion exchanger involved in iodide translocation from the cell to the colloid in the thyroid gland, and responsible for the conditioning of the endolymphatic fluid in the inner ear. Malfunction of the protein leads to Pendred syndrome, a disease complex characterized by deafness and impaired iodide organification. Here we show, that the SLC26A4 induced chloride uptake in HEK293-Phoenix cells competes with iodide, and can be blocked by NPPB and niflumic acid, whereas DIDS is unable to reduce the SLC26A4 induced chloride uptake. Furthermore, we show for the first time a direct functional characterization of a SLC26A4 mutant (SLC26A4_{S28R}) we described recently. This mutant is transposed towards the cell membrane, but its transport capability (chloride uptake) is markedly reduced compared to wild-type SLC26A4. The functional characteristics of SLC26A4_{S28R} we described, are consistent with the clinical phenotype observed in the patient.

Acknowledgements

This work was supported by the Italian Ministry of Instruction, University and Research (MIUR, prot 2003060317), and the Austrian Science Fund (FWF: P18608-B05 and P17119-B05).

References

- 1 Everett LA, Glaser B, Beck JC, Idol JR, Buchs A, Heyman M, Adawi F, Hazani E, Nassir E, Baxevanis AD, Sheffield VC, Green ED: Pendred syndrome is caused by mutations in a putative sulphate transporter gene (PDS). *Nat Genet* 1997;17:411-422.
- 2 Mount DB, Romero MF: The SLC26 gene family of multifunctional anion exchangers. *Pflugers Arch* 2004;447:710-721.
- 3 Aravind L, Koonin EV: The STAS domain - a link between anion transporters and antisigma-factor antagonists. *Curr Biol* 2000;10:R53-R55.
- 4 Royaux IE, Suzuki K, Mori A, Kato R, Everett LA, Kohn LD, Green ED: Pendrin, the protein encoded by the Pendred syndrome gene (PDS), is an apical porter of iodide in the thyroid and is regulated by thyroglobulin in FRTL-5 cells. *Endocrinology* 2000;141:839-845.
- 5 Gillam MP, Sidhaye AR, Lee EJ, Rutishauser J, Stephan CW, Kopp P: Functional characterization of pendrin in a polarized cell system Evidence for pendrin-mediated apical iodide efflux. *J Biol Chem* 2004;279:13004-13010.
- 6 Blons H, Feldmann D, Duval V, Messaz O, Denoyelle F, Loundon N, Sergout-Allaoui A, Houang M, Duriez F, Lacombe D, Delobel B, Leman J, Catros H, Journel H, Drouin-Garraud V, Obstoy MF, Toutain A, Oden S, Toublanc JE, Couderc R, Petit C, Garabedian EN, Marlin S: Screening of SLC26A4 (PDS) gene in Pendred's syndrome: a large spectrum of mutations in France and phenotypic heterogeneity. *Clin Genet* 2004;66:333-340.
- 7 Phelps PD, Coffey RA, Trembath RC, Luxon LM, Grossman AB, Britton KE, Kendall-Taylor P, Graham JM, Cadge BC, Stephens SG, Pembrey ME, Reardon W: Radiological malformations of the ear in Pendred syndrome. *Clin Radiol* 1998;53:268-273.
- 8 Fugazzola L, Mannavola D, Cerutti N, Maghnie M, Pagella F, Bianchi P, Weber G, Persani L, Beck-Peccoz P: Molecular analysis of the Pendred's syndrome gene and magnetic resonance imaging studies of the inner ear are essential for the diagnosis of true Pendred's syndrome. *J Clin Endocrinol Metab* 2000;85:2469-2475.
- 9 Fugazzola L, Cerutti N, Mannavola D, Crino A, Cassio A, Gasparoni P, Vannucchi G, Beck-Peccoz P: Differential diagnosis between Pendred and pseudo-Pendred syndromes: clinical, radiologic, and molecular studies. *Pediatr Res* 2002;51:479-484.
- 10 Morgan RA, Couture L, Elroy-Stein O, Ragheb J, Moss B, Anderson WF: Retroviral vectors containing putative internal ribosome entry sites: development of a polycistronic gene transfer system and applications to human gene therapy. *Nucleic Acids Res* 1992;20:1293-1299.
- 11 Arturi F, Russo D, Bidart JM, Scarpelli D, Schlumberger M, Filetti S: Expression pattern of the pendrin and sodium/iodide symporter genes in human thyroid carcinoma cell lines and human thyroid tumors. *Eur J Endocrinol* 2001;145:129-135.
- 12 Porra V, Bernier-Valentin F, Trouttet-Masson S, Berger-Dutrieux N, Peix JL, Perrin A, Selmi-Ruby S, Rousset B: Characterization and semiquantitative analyses of pendrin expressed in normal and tumoral human thyroid tissues. *J Clin Endocrinol Metab* 2002;87:1700-1707.
- 13 Pang XP, Hershman JM, Chung M, Pekary AE: Characterization of tumor necrosis factor-alpha receptors in human and rat thyroid cells and regulation of the receptors by thyrotropin. *Endocrinology* 1989;125:1783-1788.
- 14 Kimmich GA: Preparation and Characterization of Isolated Intestinal Epithelial Cells and Their Use in Studying Intestinal Transport; in Kor C, Plenum Press (eds): *Methods in Membrane Biology*. New York, 1975, vol IV, pp 51-115.
- 15 Bonnici B, Wagner CA: Postnatal expression of transport proteins involved in acid-base transport in mouse kidney. *Pflugers Arch* 2004;448:16-28.
- 16 Verlander JW, Hassell KA, Royaux IE, Glapion DM, Wang ME, Everett LA, Green ED, Wall SM: Deoxycorticosterone upregulates PDS (Slc26a4) in mouse kidney: role of pendrin in mineralocorticoid-induced hypertension. *Hypertension* 2003;42:356-362.
- 17 Wall SM, Hassell KA, Royaux IE, Green ED, Chang JY, Shipley GL, Verlander JW: Localization of pendrin in mouse kidney. *Am J Physiol Renal Physiol* 2003;284:F229-F241.
- 18 Kim YH, Kwon TH, Frische S, Kim J, Tisher CC, Madsen KM, Nielsen S: Immunocytochemical localization of pendrin in intercalated cell subtypes in rat and mouse kidney. *Am J Physiol Renal Physiol* 2002;283:F744-F754.
- 19 Royaux IE, Wall SM, Karniski LP, Everett LA, Suzuki K, Knepper MA, Green ED: Pendrin, encoded by the Pendred syndrome gene, resides in the apical region of renal intercalated cells and mediates bicarbonate secretion. *Proc Natl Acad Sci U S A* 2001;98:4221-4226.
- 20 Soleimani M, Greeley T, Petrovic S, Wang Z, Amlal H, Kopp P, Burnham CE: Pendrin: an apical Cl⁻/OH⁻/HCO₃⁻ exchanger in the kidney cortex. *Am J Physiol Renal Physiol* 2001;280:F356-F364.
- 21 Scott DA, Wang R, Kreman TM, Sheffield VC, Karniski LP: The Pendred syndrome gene encodes a chloride-iodide transport protein. *Nat Genet* 1999;21:440-443.
- 22 Scott DA, Karniski LP: Human pendrin expressed in *Xenopus laevis* oocytes mediates chloride/formate exchange. *Am J Physiol Cell Physiol* 2000;278:C207-C211.
- 23 Mysyna S, Lang PA, Kempe DS, Kaiser S, Huber SM, Wiedner T, Lang F: Cl⁻ channel blockers NPPB and niflumic acid blunt Ca(2⁺)-induced erythrocyte 'apoptosis'. *Cell Physiol Biochem* 2004;14:241-248.
- 24 Coelho RR, Souza EP, Soares PM, Meireles AV, Santos GC, Scarpato HC, Assreuy AM, Criddle DN: Effects of chloride channel blockers on hypotonicity-induced contractions of the rat trachea. *Br J Pharmacol* 2004;141:367-373.
- 25 Kim SJ, Shin SY, Lee JE, Kim JH, Uhm DY: Ca²⁺-activated Cl⁻ channel currents in rat ventral prostate epithelial cells. *Prostate* 2003;55:118-127.
- 26 Dou H, Xu J, Wang Z, Smith AN, Soleimani M, Karet FE, Greinwald JH, Jr, Choo D: Co-expression of Pendrin, Vacuolar H⁺-ATPase {alpha}4-Subunit and Carbonic Anhydrase II in Epithelial Cells of the Murine Endolymphatic Sac. *J Histochem Cytochem* 2004;52:1377-1384.
- 27 Royaux IE, Belyantseva IA, Wu T, Kachar B, Everett LA, Marcus DC, Green ED: Localization and functional studies of pendrin in the mouse inner ear provide insight about the etiology of deafness in Pendred syndrome. *J Assoc Res Otolaryngol* 2003;4:394-404.
- 28 van Adelsberg JS, Edwards JC, al-Awqati Q: The apical Cl⁻/HCO₃⁻ exchanger of beta intercalated cells. *J Biol Chem* 1993;268:11283-11289.
- 29 al-Awqati Q, Vijayakumar S, Takito J: Terminal differentiation of epithelia from trophoctoderm to the intercalated cell: the role of hensin. *J Am Soc Nephrol* 2003;14:S16-S21.
- 30 Wall SM: Recent advances in our understanding of intercalated cells. *Curr Opin Nephrol Hypertens* 2005;14:480-484.
- 31 Petrovic S, Wang Z, Ma L, Soleimani M: Regulation of the apical Cl⁻/HCO₃⁻ exchanger pendrin in rat cortical collecting duct in metabolic acidosis. *Am J Physiol Renal Physiol* 2003;284:F103-F112.

- 32 Schwartz GJ, Barasch J, al-Awqati Q: Plasticity of functional epithelial polarity. *Nature* 1985;318:368-371.
- 33 Schwartz GJ, Tsuruoka S, Vijayakumar S, Petrovic S, Mian A, al-Awqati Q: Acid incubation reverses the polarity of intercalated cell transporters, an effect mediated by hensin. *J Clin Invest* 2002;109:89-99.
- 34 Dunn JT, Dunn AD: Update on intrathyroidal iodine metabolism. *Thyroid* 2001;11:407-414.
- 35 Kohn LD, Suzuki K, Nakazato M, Royaux I, Green ED: Effects of thyroglobulin and pendrin on iodide flux through the thyrocyte. *Trends Endocrinol Metab* 2001;12:10-16.
- 36 Taylor JP, Metcalfe RA, Watson PF, Weetman AP, Trembath RC: Mutations of the PDS gene, encoding pendrin, are associated with protein mislocalization and loss of iodide efflux: implications for thyroid dysfunction in Pendred syndrome. *J Clin Endocrinol Metab* 2002;87:1778-1784.
- 37 Chambard JM, Ashmore JF: Sugar transport by mammalian members of the SLC26 superfamily of anion-bicarbonate exchangers. *J Physiol* 2003;550:667-677.
- 38 Ko SB, Shcheynikov N, Choi JY, Luo X, Ishibashi K, Thomas PJ, Kim JY, Kim KH, Lee MG, Naruse S, Muallem S: A molecular mechanism for aberrant CFTR-dependent HCO₃⁻ transport in cystic fibrosis. *EMBO J* 2002;21:5662-5672.
- 39 Yoshida A, Hisatome I, Taniguchi S, Sasaki N, Yamamoto Y, Miake J, Fukui H, Shimizu H, Okamura T, Okura T, Igawa O, Shigemasa C, Green ED, Kohn LD, Suzuki K: Mechanism of iodide/chloride exchange by pendrin. *Endocrinology* 2004;145:4301-4308.
- 40 Dossena S, Maccagni A, Vezzoli V, Bazzini C, Garavaglia ML, Meyer G, Furst J, Ritter M, Fugazzola L, Persani L, Zorowka P, Storelli C, Beck-Peccoz P, Botta G, Paulmichl M: The expression of wild-type pendrin (SLC26A4) in human embryonic kidney (HEK 293 Phoenix) cells leads to the activation of cationic currents. *Eur J Endocrinol* 2005;153:693-699.
- 41 Wagner CA, Finberg KE, Stehberger PA, Lifton RP, Giebisch GH, Aronson PS, Geibel JP: Regulation of the expression of the Cl⁻/anion exchanger pendrin in mouse kidney by acid-base status. *Kidney Int* 2002;62:2109-2117.
- 42 Frische S, Kwon TH, Frokiar J, Madsen KM, Nielsen S: Regulated expression of pendrin in rat kidney in response to chronic NH₄Cl or NaHCO₃ loading. *Am J Physiol Renal Physiol* 2003;284:F584-F593.
- 43 Wall SM, Kim YH, Stanley L, Glapion DM, Everett LA, Green ED, Verlander JW: NaCl restriction upregulates renal Slc26a4 through subcellular redistribution: role in Cl⁻ conservation. *Hypertension* 2004;44:982-987.
- 44 Suzuki K, Royaux IE, Everett LA, Mori-Aoki A, Suzuki S, Nakamura K, Sakai T, Katoh R, Toda S, Green ED, Kohn LD: Expression of PDS/Pds, the Pendred syndrome gene, in endometrium. *J Clin Endocrinol Metab* 2002;87:938.
- 45 Rotman-Pikielny P, Hirschberg K, Maruvada P, Suzuki K, Royaux IE, Green ED, Kohn LD, Lippincott-Schwartz J, Yen PM: Retention of pendrin in the endoplasmic reticulum is a major mechanism for Pendred syndrome. *Hum Mol Genet* 2002;11:2625-2633.
- 46 Shepshelovich J, Goldstein-Magal L, Globerson A, Yen PM, Rotman-Pikielny P, Hirschberg K: Protein synthesis inhibitors and the chemical chaperone TMAO reverse endoplasmic reticulum perturbation induced by overexpression of the iodide transporter pendrin. *J Cell Sci* 2005;118:1577-1586.
- 47 Yoshida A, Taniguchi S, Hisatome I, Royaux IE, Green ED, Kohn LD, Suzuki K: Pendrin is an iodide-specific apical porter responsible for iodide efflux from thyroid cells. *J Clin Endocrinol Metab* 2002;87:3356-3361.
- 48 Rillema JA, Hill MA: Prolactin regulation of the pendrin-iodide transporter in the mammary gland. *Am J Physiol Endocrinol Metab* 2003;284:E25-E28.
- 49 Chernova MN, Jiang L, Shmukler BE, Schweinfest CW, Blanco P, Freedman SD, Stewart AK, Alper SL: Acute regulation of the SLC26A3 congenital chloride diarrhoea anion exchanger (DRA) expressed in Xenopus oocytes. *J Physiol* 2003;549:3-19.
- 50 Faggiano A, Coulot J, Bellon N, Talbot M, Caillou B, Ricard M, Bidart JM, Schlumberger M: Age-dependent variation of follicular size and expression of iodine transporters in human thyroid tissue. *J Nucl Med* 2004;45:232-237.
- 51 Rodriguez AM, Perron B, Lacroix L, Caillou B, Leblanc G, Schlumberger M, Bidart JM, Pourcher T: Identification and characterization of a putative human iodide transporter located at the apical membrane of thyrocytes. *J Clin Endocrinol Metab* 2002;87:3500-3503.
- 52 Scott DA, Wang R, Kreman TM, Andrews M, McDonald JM, Bishop JR, Smith RJ, Karniski LP, Sheffield VC: Functional differences of the PDS gene product are associated with phenotypic variation in patients with Pendred syndrome and non-syndromic hearing loss (DFNB4). *Hum Mol Genet* 2000;9:1709-1715.